Protoplasma (2016) 253:487–501
DOI 10.1007/s00709-015-0827-0

ORIGINAL ARTICLE

Toward establishing a morphological and ultrastructural characterization of proembryogenic masses and early somatic embryos of *Araucaria angustifolia* (Bert.) O. Kuntze

Neusa Steiner[1] · Francine L. Farias-Soares[2] · Éder C. Schmidt[3] · Maria L. T. Pereira[4] · Bruna Scheid[4] · Gladys D. Rogge-Renner[3,7] · Zenilda L. Bouzon[3,5] · Daniela Schmidt[4] · Sara Maldonado[6] · Miguel P. Guerra[4]

Received: 30 January 2015 / Accepted: 30 April 2015 / Published online: 13 May 2015

Abstract Somatic embryogenesis is a morphogenetic route useful for the study of embryonic development, as well as the large-scale propagation of endangered species, such as the Brazilian pine (*Araucaria angustifolia*). In the present study, we investigated the morphological and ultrastructural organization of *A. angustifolia* somatic embryo development by means of optical and electron microscopy. The proembryogenic stage was characterized by the proliferation of proembryogenic masses (PEMs), which are cellular aggregates composed of embryogenic cells (ECs) attached to suspensor-like cells (SCs). PEMs proliferate through three developmental stages, PEM I, II, and III, by changes in the number of ECs and SCs. PEM III-to-early somatic embryo (SE) transition was characterized by compact clusters of ECs growing out of PEM III, albeit still connected to it by SCs. Early SEs showed a dense globular embryonic mass (EM) and suspensor region (SR) connected by embryonic tube cells (TCs). By comparison, early somatic and zygotic embryos showed similar morphology. ECs are round with a large nucleus, nucleoli, and many cytoplasmic organelles. In contrast, TCs and SCs are elongated and vacuolated with cellular dismantling which is associated with programmed cell death of SCs. Abundant starch grains were observed in the TCs and SCs, while proteins were more abundant in the ECs. Based on the results of this study, a fate map of SE development in *A. angustifolia* is, for the first time, proposed. Additionally, this study shows the cell biology of SE development of this primitive gymnosperm which may be useful in evolutionary studies in this area.

Keywords Somatic embryogenesis · Histochemistry · Pluripotency · Suspensor cell · Conifers

Handling Editor: Peter Nick

Neusa Steiner and Francine L. Farias-Soares contributed equally to this work.

✉ Neusa Steiner
neusa.steiner@ufsc.br

[1] Plant Physiology Laboratory, Department of Botany, Federal University of Santa Catarina, Florianópolis, SC 88040-900, Brazil

[2] Graduate Program in Plant Genetic Resources, Department of Plant Science, Federal University of Santa Catarina, C.P. 476, Florianópolis, SC 88040-900, Brazil

[3] Plant Cell Biology Laboratory, Department of Cell Biology, Embryology and Genetics, Federal University of Santa Catarina, C.P. 476, Florianópolis, SC 88049-900, Brazil

[4] Laboratory of Plant Developmental Physiology and Genetics, Department of Plant Science, Federal University of Santa Catarina, C.P. 476, Florianópolis, SC 88040-900, Brazil

[5] Central Laboratory of Electron Microscopy, Federal University of Santa Catarina, Florianópolis, SC, Brazil

[6] Departamento de Biodiversidad y Biología Experimental, Facultad de Ciencias Exactas y Naturales, Universidad de Buenos Aires, Intendente Guiraldes 2160, Pab. 2, Ciudad Universitaria, C1428EGA Buenos Aires, Argentina

[7] Department of Biological Sciences, University of Joinville Region, Joinville, SC, Brazil

Abbreviations

ABA	Abscisic acid
CA	Cytochemical analysis
CBB	Coomassie Brilliant Blue
CLSM	Confocal laser scanning microscopy
DAPI	4′,6-Diamidino-2-phenylindole dihydrochloride
ECs	Embryogenic cells
EM	Embryonic mass
FLD	Fluridone
LM	Light microscopy
PAS	Periodic acid-Schiff
PCD	Programmed cell death
PEG	Polyethylene glycol 3350
PEM	Proembryogenic mass
PEMs	Proembryogenic masses
PGRs	Plant growth regulators
SCs	Suspensor-like cells
SR	Suspensor region
SE	Somatic embryo
SEM	Scanning electron microscopy
TB-O	Toluidine blue
TCs	Embryonic tube cells
TEM	Transmission electron microscopy

Introduction

Araucaria angustifolia (Bert.) O. Kuntze is a native conifer of Brazil (Guerra et al. 2008). As a result of unsustainable exploitation and a reduction in their distribution area for agriculture or forestry, this species is one the most endangered conifers, according to the International Union of Conservation of Nature Red List of Threatened Species (2013). *A. angustifolia* seeds are recalcitrant (Farias-Soares et al. 2013), which is a bottleneck to the establishment of seed banks for ex situ conservation (Steiner et al. 2008; Jaskowiak 2014). Nowadays, for forests, the main concern is to develop strategies that allow improving the conservation of plant genetic resources by merging socioeconomic and ecological aspects of endangered species (Geburek and Konrad 2008; Global Strategy for Plant Conservation 2014). Somatic embryogenesis is a biotechnological tool for in vitro propagation and can be applied for ex situ conservation and breeding programs of woody plants (Steiner et al. 2008; Stefenon et al. 2009; Winkelmann 2013). Many economically important conifer species, such as *Picea abies* (Linneaus) (von Arnold et al. 2002), *Pinus taeda* (Linneaus) (Pullman and Bucalo 2011), and *Pinus sylvestris* (Linneaus) (Abrahamsson et al. 2012), as well as endangered species, such as *Torreya taxifolia* (Arnott) (Ma et al. 2012), *Pinus armandii* (Franchet) (Maruyama et al. 2007), and *Cedrus libani* (A. Rich.) (Khuri et al. 2000), have been propagated by somatic embryogenesis.

Somatic embryogenesis is useful from a practical point of view and as a model system for the study of morphological, cellular, physiological, and molecular events that occur during embryonic development in plants (Verdeil et al. 2007; Steiner et al. 2012; Santa-Catarina et al. 2013). Plant regeneration via somatic embryogenesis in conifers involves a sequence of steps: initiation and proliferation of embryogenic cultures, followed by early and late somatic embryo development in prematuration and maturation stages, respectively, and, finally, the maturation of somatic embryos and the development of plants (von Arnold et al. 2002; von Arnold and Clapham 2008). In this group of plants, *Picea abies* represents a model system for the development of somatic embryos (Filonova et al. 2000a; von Arnold et al. 2002). Embryogenic cultures of *Picea abies* are composed of proembryogenic masses (PEMs), which advance toward early and late somatic embryos (SEs) by a sequential series of modifications in cellular organization resembling zygotic embryo development (Filonova et al. 2000a; von Arnold et al. 2002).

Morphological and cellular analyses have been performed in several plant biological systems aimed at finding parameters to identify developmental stages and cell competence (Verdeil et al. 2001, 2007; Filonova et al. 2000a; Larsson et al. 2008a, b; Rogge-Renner et al. 2013). Pullman et al. (2003) developed a staging system in loblolly pine (*Pinus taeda*) to comparatively evaluate morphological development in zygotic and SEs. Recently, studies in Scots pine (*Pinus sylvestris*) compared the developmental pathways of SEs with normal and abnormal morphology (Abrahamsson et al. 2012). In this species, the fate map of SE development was described, and it was suggested that the presence of supernumerary suspensor cells in early SEs was caused by a disturbance in polar auxin transport, resulting in aberrant embryo development. Aberrant embryo morphology was also observed in Norway spruce 1-*N*-naphthylphthalamic acid (NPA)-treated SEs as a consequence of blocked polar auxin transport (Larsson et al. 2008a). Additionally, cytological organization has been associated with the concept of cell competence in plant stem cells. It was reported that morphological and ultrastructural analysis provides intercellular and intracellular characteristics distinguishing different cell types and providing clues to inherent developmental capacities (Verdeil et al. 2007).

A. angustifolia somatic embryogenesis has been studied for many years, and the induction and proliferation of embryogenic cultures are well established (Astarita and Guerra 1998; Guerra et al. 2000; Santos et al. 2002; Silveira et al. 2002; Steiner et al. 2005). In this species, morphological organization (Steiner et al. 2005) and exogenous polyamines (PAs) (Steiner et al. 2007) have been associated with the proliferation capacity of embryogenic cultures and with proton pump activities (Dutra et al. 2013). According to Steiner et al. (2008), the morphological organization of early SEs is the main bottleneck of any *A. angustifolia* somatic embryogenesis

protocol. Recently, however, this step was improved, and it was shown that glutathione at low concentration (Vieira et al. 2012) and endogenous changes in AIA, abscisic acid (ABA), and PA contents (Farias-Soares et al. 2014) were related to PEM-to-early SE transition. However, difficulties in performing this step have typically led to late and mature SEs obtained at a low frequency (Steiner et al. 2008). Additionally, several molecular analyses were carried out to identify molecular and biochemical markers of cell competence in embryogenic cultures, as well as compare somatic and zygotic embryo development (Balbuena et al. 2009; Steiner et al. 2012; Schlögl et al. 2012; Jo et al. 2013; Elbl et al. 2015).

Despite these efforts, our knowledge about the histodifferentiation of *A. angustifolia* SEs is still insufficient to allow a detailed morphological and ultrastructural characterization of embryogenic cultures. In order to efficiently regulate the formation of plants via somatic embryogenesis, it is necessary to understand how SEs develop. Accordingly, it is equally necessary to construct a fate map connecting morphological and cellular features associated with distinct developmental stages, thereby allowing the selection of cell lines and culture conditions that will improve somatic embryogenesis protocols for this species. It is from this perspective that the present study investigated the morphological, histological, and ultrastructural organization of PEM and early SEs of *A. angustifolia*. Cellular features, using optical and electron microscopy, as well as histochemical analysis, are shown here for the first time. Comparisons with early zygotic embryo development of *A. angustifolia* are presented and discussed.

Materials and methods

Culture conditions for somatic embryo development of *A. angustifolia*

Embryogenic cultures were induced in December 2009 from immature zygotic embryos, according to Steiner et al. (2005). Embryogenic cultures were then subcultured every 3 weeks to a plant growth regulator (PGR)-free BM medium (Gupta and Pullman 1991) supplemented with 30 g l^{-1} sucrose, 0.5 g l^{-1} casein hydrolysate, 1.0 g l^{-1} myo-inositol, and 1.0 g l^{-1} L-glutamine in alternating cycles between gelled (2 g l^{-1} of Phytagel®) and liquid medium. After proliferation, embryogenic cultures were subjected to preculture and prematuration treatments to obtain early SEs according to the procedures described by Farias-Soares et al. (2014). Embryogenic cultures were precultured for 4 weeks in DKM medium (von Arnold and Clapham 2008) supplemented with 0.5 g l^{-1} casein hydrolysate, 0.1 g l^{-1} myo-inositol, 30.0 g l^{-1} sucrose, 2.0 g l^{-1} Phytagel®, and 30 μM fluridone (FLD) (Riedel-de Haën, Seelze, Germany) diluted in dimethyl sulfoxide (DMSO). After this, the embryogenic cultures were subcultured in PGR-free DKM basal salts supplemented with 0.5 g l^{-1} casein hydrolysate, 0.1 g l^{-1} myo-inositol, 2 g l^{-1} Phytagel®, 90.0 g l^{-1} maltose (D-(+)-maltose monohydrate, Sigma-Aldrich, St. Louis, MO, USA) or 90.0 g l^{-1} lactose (α-lactose monohydrate, Sigma-Aldrich, St. Louis, MO, USA), and 70.0 g l^{-1} polyethylene glycol 3350 (PEG). In all steps, L-glutamine was filter-sterilized and added to the culture medium after autoclaving at 121 °C, 1.5 atm for 15 min. The pH of the culture medium was adjusted to 5.8 before adding the gelling agent. The cultures were incubated in the dark at 25±2 °C. Samples for morphological and ultrastructural analysis were collected from the induction, proliferation, and prematuration steps.

Morpho-cytochemical analyses

Samples from different steps of somatic embryogenesis were analyzed by means of double staining with acetocarmine and Evans blue (Gupta and Durzan 1987) in an Olympus BX 40 microscope equipped with the Olympus DP 40 image capture system and DP Controller software.

Light microscopy

Light microscopy (LM) analyses were carried out according to Schmidt et al. (2010). PEMs and SEs (SE) were fixed in phosphate buffer 0.1 M (pH 7.2) containing 2.5 % formaldehyde overnight at 4 °C or room temperature for 12 h. Subsequently, the samples were dehydrated in an increasing series of ethanol aqueous solutions. Then, the samples were infiltrated with Historesin (Leica Historesin, Heidelberg, Germany). Semi-thin sections (4 μm) containing the samples were submitted to different histochemical techniques. Periodic acid-Schiff (PAS) was used to identify neutral polysaccharides (Gahan 1984), toluidine blue (TB-O) 0.5 %, pH 3.0 (Merck Darmstadt, Germany), to identify acid polysaccharides (Gordon and McCandless 1973), and Coomassie Brilliant Blue (CBB) 0.4 % in Clarke's solution (Serva, Heidelberg, Germany) to identify proteins (Gahan 1984; Schmidt et al. 2010). Some of the sections were double-stained with PAS + CBB (Schmidt et al. 2012). Controls consisted of sections treated with the solutions without the staining component (e.g., omission of periodic acid in the PAS reaction). LM sections were analyzed using Olympus BX 40 microscopy equipped with the Olympus DP 40 image capture system and DP Controller software.

Transmission electron microscopy

PEMs and SEs were fixed in 0.1 M sodium cacodylate buffer (pH 7.2) containing 4 % formaldehyde and 2.5 % glutaraldehyde for 12 h (Schmidt et al. 2012). The material was

dehydrated in an increasing series of acetone aqueous solutions and then embedded in Spurr's resin (Spurr 1969). Ultrathin sections (70 nm) were collected on grids and stained with aqueous uranyl acetate followed by lead citrate. Two grids were then examined in the JEM 1011 transmission electron microscopy (TEM) (JEOL Ltd., Tokyo, Japan) at 80 kV.

Scanning electron microscopy

PEMs and SEs were fixed for scanning electron microscopy (SEM) observation in a manner similar to that described for TEM. The material was post-fixed with 0.1 M sodium cacodylate buffer containing 1 % osmium tetroxide for 4 h. The samples were also dehydrated in an ethanolic series, dried in the CO_2 critical point dryer (EM-CPD-030; Leica, Heidelberg, Germany), and gold sputter-coated prior to examination (Hayat 1978, modified in Schmidt et al. 2012) in the JSM 6390 LV SEM (JEOL Ltd., Tokyo, Japan) at 10 kV.

Confocal laser scanning microscopy

PEMs and SEs were analyzed under laser scanning confocal microscopy (Leica TCS SP-5, Wetzlar, Germany), using a Leica HCX PLAPO lambda ×63/1.4–0.6 oil immersion objective. For nuclei detection, 0.5 mg ml^{-1} 4′,6-diamidino-2-phenylindole dihydro-chloride (DAPI; Sigma-Aldrich, St. Louis, MO, USA) was added to the samples during 50 min (Ouriques and Bouzon 2008) and observed using a UV light-emitting diode (peak wavelength of 405-nm excitation and spectrum emission of 510–566 nm). The LAS AF Lite program (Leica) was used for final processing of the confocal images.

Results

Characterization of proembryogenic masses

Observations under light microscopy and histochemistry

Induction of embryogenic culture of *A. angustifolia* was characterized by the extrusion of a friable and translucent group of cells from the apical region of zygotic embryo (ZE) (Fig. 1a). About 30 days after extrusion, this group of cells was "budded off" from the original explant (Fig. 1b). By cytochemical analyses, embryogenic cultures were observed to be composed of two cell types: embryogenic cells (ECs), which are round, densely cytoplasmic cells, and suspensor-like cells (SCs), which are elongated, according to their degree of vacuolation (Fig. 1c). ECs stain bright red with acetocarmine, whereas SCs are permeable to Evans blue (Fig. 1c–f). These cells are attached to each other in aggregates called proembryogenic masses (PEMs). Three developmental stages of PEMs were observed: PEM I, aggregates of small groups of ECs linked to one or two SCs (Fig. 1d); PEM II, which differs from PEM I by the higher number of aggregates of ECs and increased numbers of SCs (Fig. 1e); and PEM III, which consists of large clusters of ECs and SCs without polarity (Fig. 1f). Histological analyses showed that ECs and SCs arose from the apical part of ZE (Fig. 2a). The group of round ECs is surrounded by elongated SCs (Fig. 2b), giving rise to the first cell cluster. Histochemical analyses of PEM cells by TB-O staining showed an orthochromatic reaction in the cytoplasm, and metachromatic reaction in the cell wall indicated the presence of acid polysaccharides (Fig. 2c). SCs are elongated, and their nuclei are in peripheral regions of the cell (Fig. 2b, c). ECs are small and isodiametric, and their nuclei are central and large, with one or two evident nucleoli. In some cases, cells in division can be seen (Fig. 2d). Small provacuoles appeared in white in ECs, while in SCs, a large, single autolytic vacuole can be observed (Fig. 2d–g). PAS staining showed a positive reaction, indicating the presence of neutral polysaccharides in ECs and SCs (Fig. 2e, f). In the cell wall, cellulosic compounds were stained pink, and this reaction was stronger in SCs than in ECs (Fig. 2f). In the cytoplasm, starch grains were observed close to the nuclei in SC (Fig. 2e, f), also stained in pink. CBB in double staining (CBB + PAS) revealed large amount of protein in ECs, across the cell cytoplasm, nuclei, and nucleoli stained in blue (Fig. 2g, h). In SCs, the proportion of protein is lower than that of ECs, and the nuclei are located in peripheral regions (Fig. 2g).

Observations of proembryogenic masses under transmission electron microscopy

Similar to LM observations, ECs in TEM showed large central nuclei with distinguishing heterochromatin and euchromatin (Fig. 3a). Starch grains and many small provacuoles were frequently seen in the cytoplasm (Fig. 3a). The cell wall was thin with a few plasmodesmata (Fig. 3b). Several round-shaped vacuoles, mitochondria (M), rough endoplasmic reticulum (RER), Golgi bodies (G), and amyloplasts with starch grains (S) were present in the cytoplasm (Fig. 3c). In the cytoplasm of some SC nuclei, starch grains and vacuoles were observed (Fig. 3d). However, most SCs were devoid of these organelles, and similar to LM analysis, only a large vacuole was observed (Fig. 3d).

Observations of proembryogenic masses under scanning electron microscopy and confocal laser scanning microscopy

SEM analyses revealed clusters of ECs connected to SCs (Fig. 4a), forming embryogenic cultures, thus confirming the results of LM analyses. Numerous SCs with different sizes and shapes were observed, many of them resembling "empty long balloons," resulting in a very irregular surface

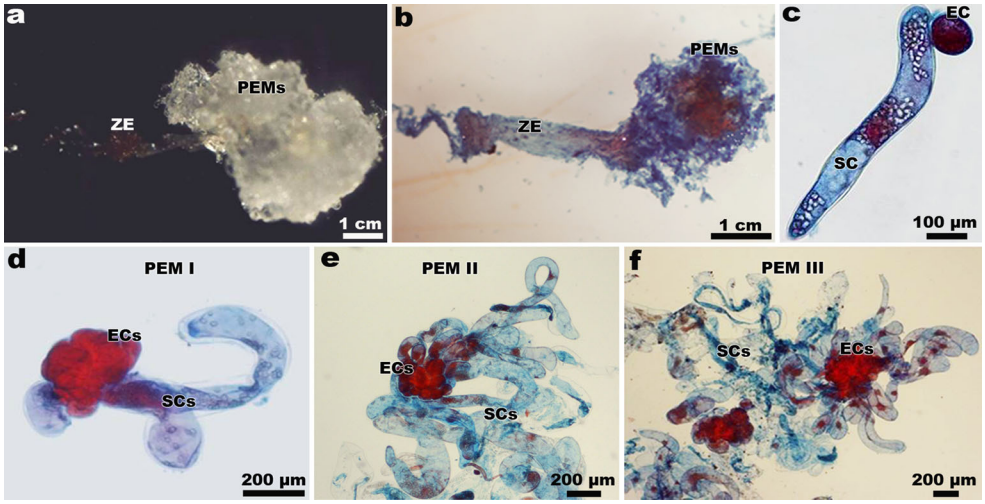

Fig. 1 Light microscopy and morpho-cytochemical analyses with acetocarmine and Evans blue of embryogenic culture of *A. angustifolia*. **a** Induction of embryogenic culture composed of proembryogenic masses (*PEMs*) from zygotic embryo (*ZE*). **b** Extrusion of PEMs from apical region of ZE. **c** Embryogenic cells (*ECs*) stained by acetocarmine and suspensor-like cells (*SCs*) stained by Evans blue. Note the presence of nucleus stained by acetocarmine in SCs. **d**–**f** Proembryogenic masses (PEMs) in three developmental stages: **d** proembryogenic mass I (*PEM I*) composed of a group of ECs linked to one or two SCs, **e** PEM II that differs from PEM I by the higher number of aggregates of ECs and increased number of SCs, and **f** PEM III with large clusters of ECs connected to SCs

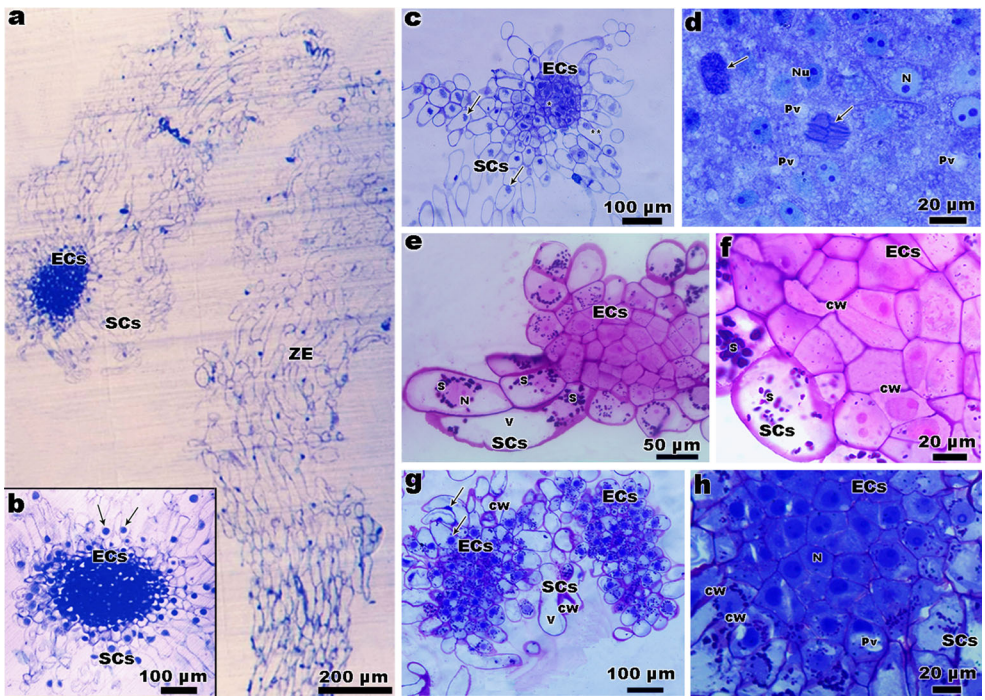

Fig. 2 Light microscopy and histochemical analyses of the induction and development of proembryogenic masses (PEMs) in *A. angustifolia*. **a** Induction of PEMs stained by TB-O with embryogenic cells (*ECs*) and suspensor-like cells (*SCs*) originated from the apical part of zygotic embryo (*ZE*). Note the presence of elongated suspensor region (SR) composed of SCs in the ZE basal part. **b** Detail of apical part of ZE with the rise of ECs surrounded by vacuolated and nucleated suspensor-like cells (*SCs*) stained by TB-O. **c** PEM II stained by TB-O with a group of ECs surrounded by SCs. Note an orthochromatic reaction in the cytoplasm (*arrow*) and metachromatic reaction in the cell wall (CW), indicating the presence of acid polysaccharides (*arrow*). **d** ECs indicating high mitotic activity. Observe different phases of cell division (*arrows*). A rather bulky nucleus (*N*) is observed with predominantly heterochromatic regions and one or two large nucleoli (*Nu*) evident by AT-O staining. **e** Sections of PEM II stained with PAS. Note the presence of a large amount of starch grains (*S*) close to the nucleus (*N*) in the vacuolated SCs. **f** Detail of ECs with small starch grains and cellulosic compounds in the cell wall (*CW*), as revealed by PAS staining. **g** Double staining (PAS + CBB) of PEM III showed large vacuoles (*V*) in SCs, and in **h** ECs, intense blue was observed, evidencing a large amount of protein organelles and large nucleus (*N*). **g**–**h** Proteins are marked in *blue* and cell wall (*CW*) in *pink*

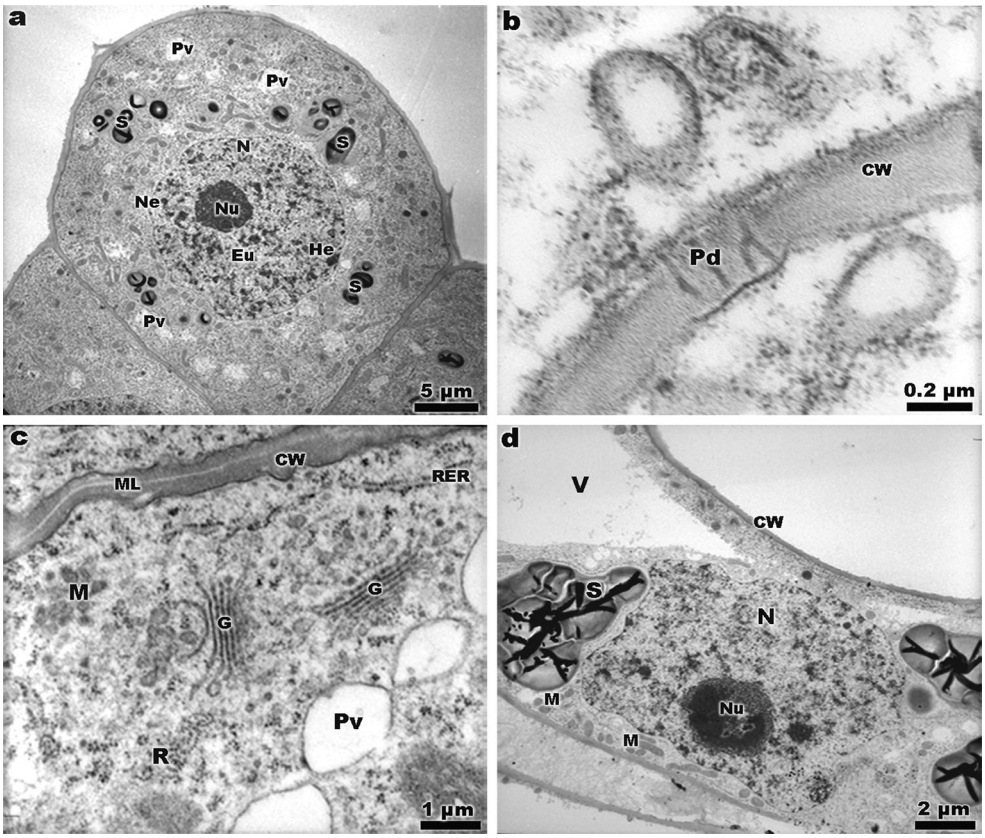

Fig. 3 Transmission electron microscopy images of *A. angustifolia* proembryogenic masses (PEMs). **a** Embryogenic cells (ECs) with nucleoli (*Nu*) and nuclei (*N*) with heterochromatin (*He*) and euchromatin (*Eu*) regions and nuclear envelope (*Ne*). Note also the presence of pro-vacuoles (*Pv*) and amyloplast with starch grains (*S*). **b** Detail of cell wall (*CW*) with the presence of plasmodesmata (*Pd*). **c** Cytoplasm of ECs with the presence of Golgi bodies (*G*), rough endoplasmic reticulum (*RER*), provacuoles (*Pv*), mitochondria (*M*), and ribosomes (*R*). Observe the cell wall (*CW*) and the middle lamella (*ML*). **d** Suspensor cells (SCs) with the presence of nucleus (*N*), nucleoli (*Nu*), amyloplast with starch grains (*S*), mitochondria (*M*), and vacuoles (*V*)

topography (Fig. 4a). Using this technique, ECs were less evident than SCs (Fig. 4a). In embryogenic culture, nuclei reacted to DAPI, featuring a single large central and active nucleus (Fig. 4b). Some SCs reacted to DAPI, and the nucleus could be observed (Fig. 4c).

Characterization of early somatic embryos

Observations under light microscopy and histochemistry

Following FLD preculture, prematuration treatment with PEG and maltose stimulated the differentiation of early SEs from PEM III (Farias-Soares et al. 2014). PEM III-to-early SE transition was characterized by compact clusters of ECs growing out of PEM III, albeit still connected to it by SCs (Fig. 5a, b). PEM-to-SE transition was not observed from PEM I or II, but only from PEM III. This stage was observed to be the starting point of early SEs (Fig. 5b). After transition, early SEs were characterized by an individualized structure composed of two polarized regions: a dense globular embryonic mass (EM) connected to a suspensor region (SR) (Fig. 5c, e, f). The EM was composed of ECs, and the SR was composed of SCs (Fig. 5c). At this stage, a transitional region was observed between EM and SR, as shown by acetocarmine and Evans blue staining (Fig. 5c, e, f). The cells located just below EM

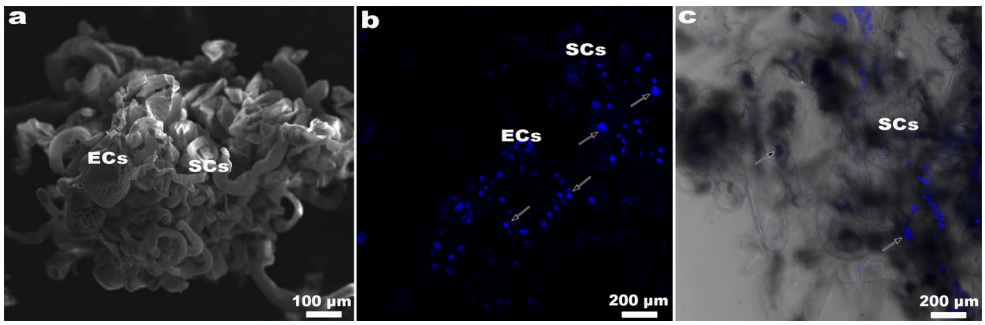

Fig. 4 Scanning electron microscopy and confocal laser scanning microscopy images of *A. angustifolia* proembryogenic masses III (PEM III). **a** PEM III with elongated suspensor cells (*SCs*) and a few embryogenic cells (*ECs*) without polarity. **b** Overview of PEM III with nucleus (N) stained with DAPI (*arrows*). **c** Note large nuclei in some suspensor cells (*SCs*) (*arrows*)

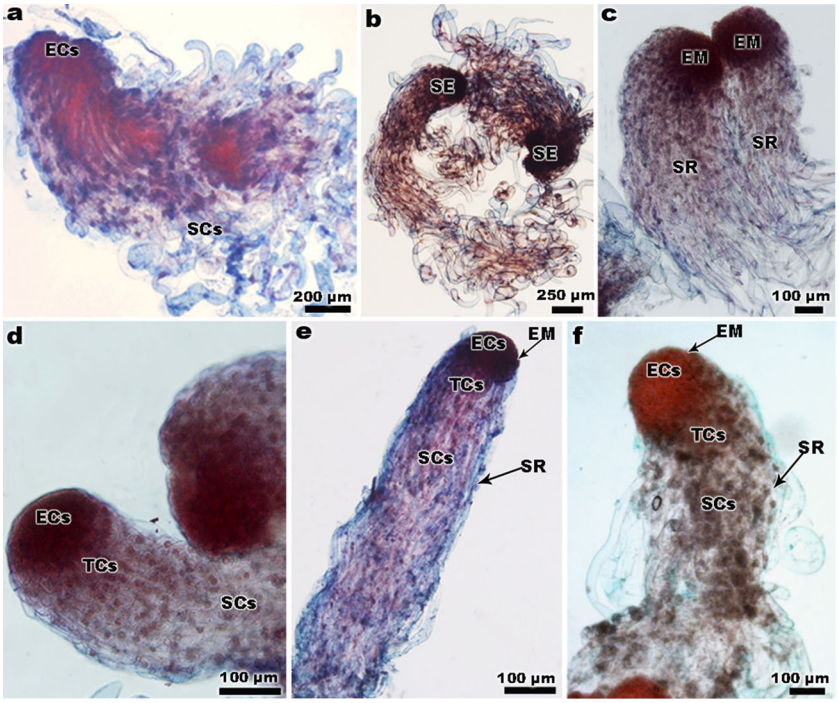

Fig. 5 Light microscopy and morpho-cytochemical analysis with acetocarmine and Evans blue of early somatic and zygotic embryos of *A. angustifolia*. **a** PEM III-to-early somatic embryo (SE) transition. Note the beginning of polarization, as indicated by a compact cluster of ECs growing out of PEM III, albeit still connected to it by SCs. **b** Multiple individualized early SEs emerging from PEM III. **c** Early SE polarized with an embryonic mass (*EM*) and suspensor region (*SR*). **d** In early SE, observe the presence of the embryogenic cells (*ECs*) in the EM stained red and suspensor-like cells (*SCs*) in the SR reactive to Evans blue. Note the presence of embryonic tube cells (*TCs*) between EM and SR. **e** Early zygotic embryos (ZEs). Observe the presence of the embryonic mass (*EM*) and suspensor region (*SR*) organized into two different regions. Note the presence of ECs, TCs, and SCs (*arrows*). **f** Early SE individualized and polarized with two regions similar to those observed in early ZE. Note the smooth surface of EM in an early SE

presented some characteristics of ECs, such as large and intact nuclei and small vacuoles. However, they showed an increase in length and became more vacuolated, similar to SCs. This is the first time that these cells have been observed in SEs of *A. angustifolia*, and our results suggest that these cells are embryonic tube cells (TCs). Also, when we performed a comparative analysis of early ZEs (Fig. 5d), the same morphological organization of early SEs was observed (Fig. 5e, f). At early embryogenesis, normal embryo development was characterized by the establishment of polarity with a distinct EM connected to a SR (Fig. 5d–f).

Using histochemical analysis with TB-O staining, all early SEs presented an opaque and compact EM region composed of ECs, a transition region with TCs, and an elongated SR composed of SCs (Fig. 6a). TB-O shows an orthochromatic reaction in cytoplasm and a metachromatic reaction on the cell wall of ECs. These are small-sized isodiametric cells with a dense cytoplasm, containing a large nucleus with one or two prominent nucleoli (Fig. 6b). PAS staining revealed a degree of starch grain deposition between EM and SR (Fig. 6c). PAS staining of TCs next to ECs showed abundant starch grains, while the starch grains in ECs were observed in lesser amounts (Fig. 6d). In SCs, cellulosic compounds were observed in the cell wall (CW), as revealed by PAS staining (Fig. 6d). In the SR, the beginning of elongation of TCs was observed, while the SCs became completely vacuolated and elongated (Fig. 6e). PAS alone or in double staining (CBB + PAS) showed a positive reaction in the CWs of ECs, while in the SCs, this reaction was stronger (Fig. 6e, f), indicating neutral polysaccharides. Abundant proteins were observed in ECs across the cell cytoplasm and nuclei assessed by staining with CBB (Fig. 6f). However, in TCs and SCs, a weak reaction to CBB was also observed, indicating a small amount of proteins, and their nuclei, when visible, were located in peripheral regions (Fig. 6f).

Observations of early somatic embryos under transmission electron microscopy

TEM analysis showed that ECs were densely cytoplasmic cells, with a central large nucleus with heterochromatin, nucleoli, and intact nuclear envelope (Fig. 7a–c). Plastids were shown to contain, or not, S, and many cytoplasmic organelles, such as M, RER, G, and small provacuoles around the nucleus were observed (Fig. 7b–c). The CW presented a uniform thickness and middle lamella associated with plasma membrane (Fig. 7d). Our results indicated that these cells are very

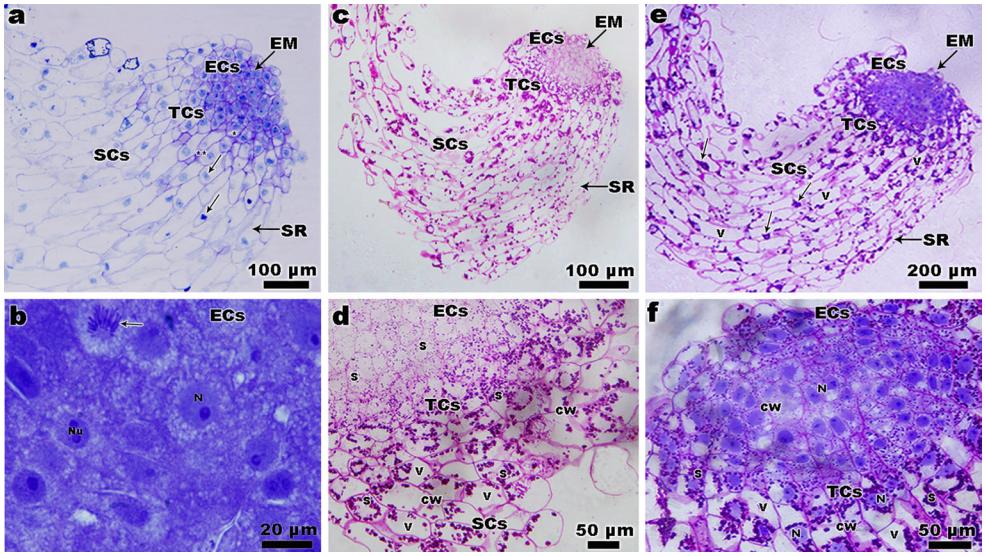

Fig. 6 Light microscopy and histochemical analyses of *A. angustifolia* early somatic embryos (SE). **a** Sections stained with TB-O of early SE with three regions: a compact embryonic mass (*EM*) composed of embryogenic cells (*ECs*), a transition region with embryonic tube cells (*TCs*), and an elongated suspensor region (*SR*) composed of many suspensor-like cells (SCs). **b** Detail of ECs from EM with a central large nucleus (*N*) with one or two nucleoli (*Nu*) and mitotic activity (*arrow*). **c** PAS staining of EM showing a bright region and the SR with a degree of starch grain (S) deposition. **d** Detail of TCs and SCs with a large amount of starch grains (*S*) present close to the nucleus (N) or in peripheral regions of the cells. Note the PAS staining of cellulosic compounds in the cell wall (*CW*). **e** Double staining (PAS + CBB) of early SE with the EM region composed of ECs and a long SR composed of TCs and SCs. **f** Detail of vacuolated TCs and SCs with nucleus (*N*) in the peripheral region and small amount of protein in *blue*. ECs double-stained by (PAS + CBB) showed a large amount of proteins marked in *blue* by CBB and a central large nucleus (*N*) with one or two prominent nucleoli (Nu)

active and contain many organelles in intense activities and proteins in cytoplasm.

Ultrastructural characterization of TCs and SCs by TEM allowed the identification of different degrees of cellular disassembly compared to cellular organizations of ECs. The first modification was the occurrence of several provacuoles around the nucleus (Fig. 7e). Apparently, the autolytic vacuole arises through engulfment of large vesicles and portions of cytoplasm by provacuoles that progressively destroy the cytosol and organelles (Fig. 7f, g). A plastolysome-like structure (Pl) was revealed as a portion of cytoplasm surrounded by one or several double membranes arising from a plastid-like leucoplast (Fig. 7h). Provacuoles increase in number and size toward the cell periphery. After the formation of large central vacuoles, the cytoplasm often occupies a narrow layer confined between tonoplast and plasma membrane (Fig. 7i). In this layer, M, amyloplasts with S, RER, G, and many vesicles from G were observed to increase according to the degree of cell dismantling (Fig. 7i, j). At the same time, many leucoplasts completely differentiate into amyloplasts (Fig. 7k), and some of these develop into etioplasts presenting prolamellar body and starch grains (Fig. 7l). A large amount of lipid bodies (LBs) was also observed at this stage (Fig. 7k).

The earliest ultrastructural sign of nuclear degradation is reflected by the normally round nucleus becoming crenulated and lobed (Fig. 7m). Dismantling of the nuclear envelope was detected by the large clusters of nuclear pore complexes (NPCs) and contents of chromatin leaking into the cytoplasm (Fig. 7n). Nuclear fragments in lobed nucleus and the increase of heterochromatin, as well as the presence of M, G, amyloplasts, and provacuoles, were observed (Fig. 7o). At the end of cellular dismantling, the autolytic vacuole occupies the entire cellular extension, and the protoplasm disappears, resulting in a cellular corpse represented by only the CW (Fig. 7p).

Observations of early somatic embryos under scanning electron microscopy and confocal laser scanning microscopy

By SEM analysis, the PEM III-to-early SE transition was observed as a prominent globular group of cells growing out of embryogenic cultures (Fig. 8a). It was possible to identify the beginning of individualization of early SEs by EM formation and elongation of SCs (Fig. 8b). After transition step, early SE individualization was observed (Fig. 8c). These embryos showed bipolar morphology similar to that observed in the cytochemical analysis. By SEM analysis, we observed a small-sized and compacted group of ECs (Fig. 8d) composed of an EM region (Fig. 8b, c). The SR region was composed of elongated SCs (Fig. 8b, c), resembling "empty balloons," and starch grains were observed inside them (Fig. 8e). By confocal laser scanning microscopy (CLSM) analysis, ECs of the EM were strongly positive to DAPI (Fig. 8f) and presented a single

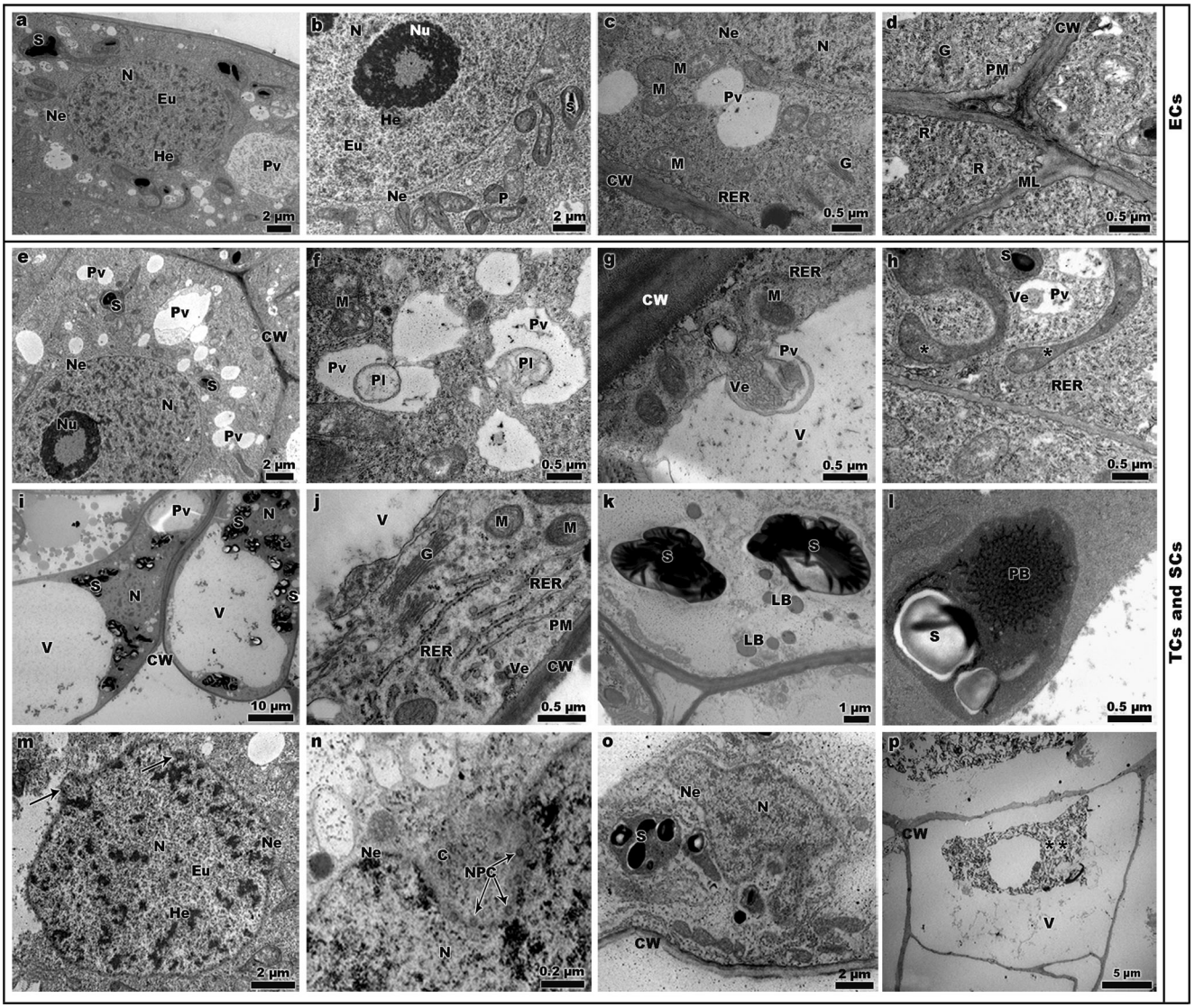

Fig. 7 Transmission electron microscopy images of *A. angustifolia* embryogenic cells (ECs), embryonic tube cells (TCs), and suspensor-like cells (SCs) of early somatic embryos (SE). **a** ECs with round nuclei (*N*) with nucleolus (*Nu*) presenting euchromatin (*Eu*) and heterochromatin (*He*) surrounded by starch grains (*S*) and provacuoles (*Pv*). **b** Detail of ECs with nuclei (*N*) with nucleolus (*Nu*) and plastids (*P*) containing, or not, starch grains (*S*) around the nuclei. **c** Detail of provacuoles (*Pv*), mitochondria (*M*), Golgi bodies (*G*) close to the nuclei (*N*) with the intact nuclear envelope (*Ne*). **d** Note the cell wall (*CW*) with middle lamella (*ML*) and uniform thickness, cytoplasm with a large amount of rough endoplasmic reticulum (*RER*), and notable plasma membrane (*PM*). **e** Beginning of tube cell dismantling, as indicated by the presence of several provacuoles (*Pv*) around the nucleus (*N*), presenting nucleoli (*Nu*) and plastids containing, or not, starch grains (S). **f** Engulfment of plastolysome-like structure (*Pl*) in provacuoles (*Pv*). **g** Engulfment of provacuoles (*Pv*) with many vesicles (*Ve*) in autolytic vacuole (*V*). Observe the presence of mitochondria (*M*). **h** Note the plastid-like leucoplast becoming a plastolysome-like structure by spoon-like extension (*asterisks*). Note rough endoplasmic reticulum (*RER*) near the leucoplast and provacuole (*Pv*) containing many vesicles (*Ve*). **i** Central large autolytic vacuole (*V*) pushing the cytoplasm with nucleus (*N*), amyloplasts with starch grains (*S*), and provacuoles (*Pv*). Observe the presence of cell wall (*CW*). **j** Detail of a small part of cytoplasm of a vacuolated (*V*) cell with Golgi bodies (*G*), rough endoplasmic reticulum (*RER*), mitochondria (*M*), and transport of vesicles (*Ve*) via cell wall (*CW*). **k** Amyloplasts with starch grains (*S*). Note the presence of lipid body (*LB*). **l** Prolamellar body (*PB*) and starch grains (*S*). **m** Round nucleus (*N*) becoming lobed nucleus (*arrow*), presenting heterochromatin (*He*) and euchromatin (*Eu*). **n** Dismantling of nuclear envelope (*Ne*), presence of nuclear pore complexes (*NPCs*, *arrows*), and contents of chromatin (*C*) in cytoplasm. **o** SCs dismantling with lobed nucleus (*N*) and amyloplast with starch grains (*S*). **p** Rupture of tonoplast leads to complete lysis of the protoplast with all cellular content (*asterisks*)

large central and active nucleus with visible nucleoli (Fig. 8g). The reaction to DAPI weakened gradually between TCs and SCs, and in some SCs, nuclei were visualized in the peripheral region of the cell (Fig. 8f).

Discussion

The present study described the morphological and ultrastructural characterization of SE development in *A. angustifolia*,

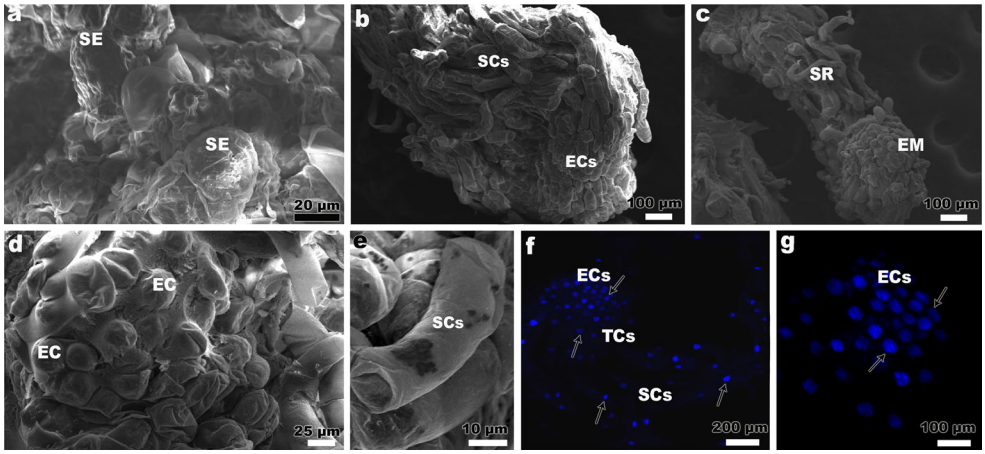

Fig. 8 Scanning electron and confocal laser scanning microscopy images of the PEM III-to-early somatic embryo (*SE*) transition and early SE of *A. angustifolia*. **a** Overview of embryogenic culture with the rise of early SE on the surface. **b** PEM-to-early somatic embryo (SE) transition with the beginning of polarity with suspensor cells (*SCs*) in the basal part and embryogenic cells (*ECs*) in the apical part. **c** Early individualized SE shows the regions of the embryonic mass (*EM*) connected to the suspensor region (*SR*). Note embryogenic cells (ECs) in EM and suspensor-like cells (SCs) in SR with slightly irregular surface topography. **d** Detail of embryogenic cells (*ECs*) and **e** suspensor-like cells (*SCs*) resembling "empty balloons" with starch grains (S) observed inside. **f** ECs from EM present a strong reaction of the nucleus with DAPI (*arrows*), decreasing gradually between embryonic tube cells (TCs) and suspensor-like cells (SCs). Note large and central nucleus in ECs and few nuclei in the TCs and SCs. **g** Detail of ECs with a single large central nucleus (N) (*arrows*)

beginning with the induction of the PEMs from ZEs, which, in its most advanced stage, PEM III, gives rise to early SE. The morphological characterization allows us to identify two stages of development in *A. angustifolia* SEs: proembryogenic and early embryogenic.

Plant embryo development can be divided into two main steps: embryogenesis sensu stricto and maturation of the embryo, followed by germination (Dodeman et al. 1997). The sequence of embryo development in gymnosperms can be divided into three phases (Singh 1978): (i) proembryogeny: all stages before the elongation of the suspensor, (ii) early embryogeny: all stages after elongation of the suspensor and before establishment of the root meristem, and (iii) late embryogeny: intensive histogenesis, including establishment of the root and shoot meristems (von Arnold et al. 2002; Williams 2009). These stages are similar, but not identical, to those described in angiosperm embryogenesis (Dodeman et al. 1997; Weigel and Jürgens 2002). In the present work, the proembryogenic stage was represented by proliferation of PEMs, which are cell aggregates composed of densely cytoplasmic cells called ECs, which are attached to vacuolated cells, termed SCs. According to Filonova et al. (2000a), in *Picea abies*, PEMs were classified as PEM I, consisting of cell aggregates composed of small, compact clumps of embryogenic cells adjacent to a single SC, while similar cell aggregates possessing more than one suspensor like-cell are classified as PEM II. At the PEM III stage, enlarged clumps of embryogenic cells appear looser, rather than compact, and the polarity is disturbed. This confirms our observations in *A. angustifolia*, in which PEMs also passed through three typical developmental stages with numerous ECs and SCs, and no polarity was observed. At this stage, the PEMs seem to be self-renewed through the autoreplicative capacity of ECs. A strong reaction to acetocarmine and CBB was observed in ECs; this revealed a dense cytoplasm, large nucleus, and a large amount of proteins. In contrast, the SCs showed many vacuoles and were highly permeable to Evans blue, but weakly reactive to acetocarmine and CBB. These same reactions to acetocarmine and Evans blue were previously described for embryogenic cultures of *A. angustifolia* (Steiner et al. 2005). Evans blue, as an isomer of Trypan blues, is frequently used in plant cells, passively entering through breaks in the plasma membrane of dying cells (Baker et al. 1994; Filonova et al. 2000b), marking dead or dying cells. Furthermore, CLSM analysis shows that ECs, unlike SCs, presented a nucleus highly reactive to DAPI. These characteristics are similar to those described for embryogenic cultures of *Picea abies* (Filonova et al. 2000a), *Pinus sylvestris* (Abrahamsson et al. 2012), and *Juniperus communis* (Helmersson and von Arnold 2009). The morphological organization of PEMs observed in the present work is similar to the proembryonic zygote in gymnosperms (Dogra 1978; Singh 1978; von Arnold et al. 2002). Similarly, in angiosperm species, ECs and SCs arise after the establishment of asymmetry of the first zygotic division and subsequent apical-basal patterning (Souter and Lindsey 2000; von Arnold et al. 2002). Our results confirm that the culture condition established for this step in the somatic embryogenesis protocol of *A. angustifolia* (Steiner et al. 2005, 2007, 2008) promotes the development and morphological organization of PEMs corresponding to the proembryogenic stage observed in somatic and ZE development of conifers.

However, to efficiently regulate the whole process of plant regeneration through somatic embryogenesis, it is important

to understand the early developmental events of this process. After the proembryogenic stage, PEM III advances to early SE (Filonova et al. 2000a) by the establishment of polarity. Proembryo-to-early SE embryo transition plays a pivotal role in somatic embryogenesis in conifers, and the inability of many embryogenic cultures to form well-developed embryos is, in large part, associated with disturbances in morphological and biochemical aspects that might be a consequence of inappropriate culture conditions (von Arnold et al. 2005). It was suggested that the early embryos should not be exposed to maturation treatments before they have reached the appropriate developmental stage (von Arnold et al. 2002, 2005). Both intrinsic and extrinsic signals can help to establish polarity in the early plant embryo, and this control operates in a coordinated manner during early embryogenesis (Souter and Lindsey 2000). In *Picea abies*, the induction and proliferation of PEM occurs with the presence of auxins and cytokinins, while for PEM-to-SE transition, the PGRs are withdrawn, and the complete development of early SEs requires ABA (Filonova et al. 2000a; von Arnold et al. 2002, 2005). It has been described that PEM-to-early SE transition in *Picea abies* requires a degree of morphological organization of PEMs during the proembryogenic stage (Filonova et al. 2000a) before submitting them to ABA treatment. Moreover, it was reported that this morphological organization was related to polar transport of auxin and programmed cell death (PCD) in the PEMs at proembryogenic stage (Larsson et al. 2008a, b; Abrahamsson et al. 2012). In *A. angustifolia*, the induction and proliferation of PEMs from ZEs occur in the presence or absence of auxins and cytokinins (Steiner et al. 2005, 2007, 2008), as we described previously. However, the trigger of PEM III-to-early SE transition occurred after FLD pretreatment, during the prematuration treatments, supplemented with maltose or lactose, associated, or not, with PEG, which promoted endogenous IAA, ABA, and PA changes (Farias-Soares et al. 2014).

The present work showed that these intrinsic and extrinsic signals affect morphological organization and that the PEM-to-early SE transition was characterized by the development of new globular structures from PEM III, followed by early SEs starting to differentiate. At the early embryogenesis stage in *A. angustifolia*, the two groups of cells, ECs and SCs, became polarized, forming two poles, the embryonic mass (EM) composed of ECs attached to the suspensor region (SR) formed by SCs. At this stage, the presence of partially vacuolated TCs was also observed. TCs comprise cell layers that form a transition between ECs and SCs. Compared to ZE development in conifers, this is the early embryogenesis stage, which includes all the stages after suspensor elongation, and precedes the rise of meristems (Singh 1978; von Arnold et al. 2002). So far, this is the first report describing the morphological organization of early *A. angustifolia* SE, and compared to what we observed in early ZEs, we suggest a normal SE development. Moreover, our results are similar to those observed in *Picea abies* embryo development (Singh 1978; Filonova et al. 2000a, b; von Arnold et al. 2002; 2005; Larsson et al. 2008a, b), as well as in *Pseudotsuga menziesii* (Mirb.) Franco (Durzan 2008). These authors reported that the asymmetric divisions of the most basally situated cells within the embryonic mass (EM) give rise to a layer of elongated embryonic tube cells (TCs), which differentiated to form a layer of SCs. To the best our knowledge, this layer of cells has neither been observed nor described in early SEs of *A. angustifolia*. In this work, we observed that this cell type showed characteristics of ECs, such as large and active nucleus, as well as other characteristics of SCs, such as a large number of provacuoles and starch grains. In *Picea glauca* (Moench) Voss), this pattern also occurred, having originated from the basal end of the EM (Joy et al. 1991) and leading to these authors to suggest that the SCs and basal region of the embryo play an important role in channeling nutrients. According to Helmersson et al. (2008), the SR of *Picea abies* is composed of several layers of elongated cells with increased degree of cellular disassembly, beginning with the cells committed to PCD in the first layer adjacent to the EM and continuing toward the basal end of the suspensors. Moreover, in *Picea abies* (Larsson et al. 2008a) and *Pinus sylvestris* (Abrahamsson et al. 2012), it was suggested that the unbalanced ratio between the EM and the SR results from the formation of extra suspensor cells, rather than suppression by PCD. Based on this, we can infer that the TCs present in early *A. angustifolia* SE give rise to the SCs, which can be considered the cells committed to PCD, once these cells are permeable to Evan's blue and the ultrastructural analyses showed cellular disassembly.

The histochemistry analysis revealed a similar pattern of storage product deposition in ECs and SCs at proembryogenic and early embryogenesis stages of *A. angustifolia* SE. CBB in double staining (CBB + PAS) revealed a large amount of protein in ECs across the cell cytoplasm, nuclei, and nucleoli stained in blue, while in SCs, the proportion of protein was lower. PAS staining showed a positive reaction, indicating the presence of neutral polysaccharides in ECs and SCs. A few amyloplasts were observed in ECs of the EM, but a high number of TCs and SCs of SE. The accumulation of adequate reserves in conifer SEs is vital because post-germination growth occurs in the absence of the haploid megagametophyte, which is the major storage organ in conifer seeds (Grigová et al. 2007). Based on histochemical studies, Joy et al. (1991) identified a precise pattern of storage compound accumulation during somatic embryogenesis in *P. glauca* where in starch accumulated first, followed by lipids and proteins. These authors found that starch accumulated in the proximal part of the SR during early somatic embryogenesis in a manner similar to that described in the present work. At late stage, these authors described the accumulation of starch in

the shoot pole and cortex of SE. The gradients in reserve deposition during SE development indicate that physiologically different regions are present in developing embryos and that they may be required for establishing patterns of tissue differentiation, as has been suggested to occur during apical meristem formation in ZEs (Yeung et al. 1998). Meristem cells of *A. angustifolia* cotyledonary ZEs show few starch grains (Rogge-Renner et al. 2013), and a low starch content was also found by Tereso et al. (2007) in the cotyledons of *Pinus pinaster* (Aiton) ZEs. However, the pattern of storage product deposition during in vitro embryo development is a result of such culture conditions as salt and sucrose concentrations, exogenous PGRs, osmotic environment, and lack of maternal influence (Joy et al. 1991). Considering these features, our results suggest that the greater starch deposition in SCs and proteins in ECs at proembryogenic and early stages are related to the culture condition and with the intrinsic role played by these cells in SE development. SCs play an important role in channeling nutrient transport (Joy et al. 1991), while ECs are associated with high mitotic activity, since these cells will give rise to the whole plant embryo (Weigel and Jürgens 2002).

By TEM analysis, it was possible to characterize the ultrastructure of the cells that comprise the SE of *A. angustifolia* at proembryogenic and early stages: ECs, TCs, and SCs. At both of stages, ECs present a high nucleus: cytoplasm ratio, a spherically shaped nucleus containing one or two nucleoli, and CW of uniform thickness with the presence of a few interconnecting plasmodesmata. Meristematic stem cells have a thin primary CW, and plasmodesmata connections allow intercellular movement, such as transcription factors, which control developmental processes (Haywood et al. 2002; Kurata et al. 2005). A dense cytoplasm with few G, RER, many M, some plastids, and provacuoles was also observed. According to Verdeil et al. (2007), meristematic stem cells were classified as pluripotent cells, while embryogenic cells were classified as totipotent cells. These authors reported that both pluripotent stem cells and totipotent embryogenic stem cells share certain cellular characteristics, including a high nucleus/cytoplasm ratio, a dense cytoplasm, and a small fragmented vacuome. However, these authors also reported that one distinguishing cytological characteristic of embryogenic cells is their nuclear architecture and chromatin structure. The nuclei of pluripotent meristematic stem cells are spherically shaped with several nucleoli. The nuclei of totipotent embryogenic stem cells are irregularly shaped with invaginations of the nuclear envelope and contain one large nucleolus.

Previous studies with LM and TEM analyses showed the presence of pluripotent cells in shoot and root apical meristem of *A. angustifolia* cotyledonary stage ZEs (Rogge-Renner et al. 2013). However, in the present work, we observed that ECs presented many features described by Verdeil et al. (2007) for totipotent embryogenic cells. Also, our results are similar to those observed in embryogenic cells of coconut calli in that those cells give evidence that invaginations of the nuclear envelope and the emission of Golgi vesicles could be directly related to an increase in CW thickness (Verdeil et al. 2001). However, such characteristics of pluripotent cells as high nucleus/cytoplasm proportion and highly vacuolated cytoplasm were also observed (Yeung 1995). These results therefore indicate that ECs of SE in *A. angustifolia* showed cellular characteristics of pluripotent and totipotent cells and that the localization of these ECs in EM of the SE is related to the establishment of the meristems during late stages of embryo development.

In the TEM analysis of TCs and SCs, CW thickness, nucleus with nucleoli, starch granules, and a bigger vacuole than that observed in ECs were all noted. In these cells, a degree of cellular dismantling was observed to occur gradually from TCs up to SC development. The transition from living cells to cell corpses was accompanied by changes in cell shape and cytoplasmic organization (Filonova et al. 2000a, b; Filonova et al. 2002; Smertenko et al. 2003; Klionsky et al. 2012). In the present work, we observed that one of the signals of cell dismantling is the accumulation of provacuoles and plastids around the nucleus which receives large vesicles from Golgi bodies. It was also observed that portions of cytoplasm were engulfed by provacuoles, and at the late stage of cell dismantling, the formation of a single autolytic vacuole occurs. According to Filonova et al. (2000a, b), the earliest morphological sign of PCD in the embryo suspensor is an increase in the number and activity of Golgi complexes. Autolytic vacuoles and vesicles then accumulate in the cytoplasm and form one or more large vacuoles that take up most of the cell volume (Smertenko et al. 2003). Moreover, in the present work, a plastolysome-like structure (Pl) was observed. This has been related to the programmed lysis of the suspensor cells in *Phaseolus coccineus* (Linnaeus) (Nagl 1977). These authors reported that the plastids were transformed into Pl and that these structures could be characterized as a portion of cytoplasm surrounded by one or several double membranes, with sequestered cytoplasm and increased electron translucency. Pl was also observed during the dismantling of suspensor cells in embryos of *Phaseolus vulgaris* (Linnaeus) (Gärtner and Nagl 1980) and *Picea abies* (Filonova et al. 2000b). Similar to the suggestion of Nagl (1977), our data showed that Pl arises from plastids, or, more specifically, leucoplast, and that this transformation was characterized by the extension of plastid formation. These results suggest that both Pl and provacuoles are engaged in dismantling TCs and SCs during *A. angustifolia* SE development. Concurrent with the changes in cytoplasm organization, nuclear modifications were also observed. The round nucleus becomes lobed, followed by segmentation of nuclear envelope, leaving large clusters of nuclear pore complexes (NPCs), and in some cases, increase in heterochromatin was observed. Similar characteristics were observed in autolysis of SCs in ZEs of *Phaseolus coccineus* (Nagl 1977), *Pinus*

sylvestris (Filonova et al. 2002), and SEs of *Picea abies* (Filonova et al. 2000b). According to Domínguez and Cejudo (2012), cells undergoing PCD begin a degenerative process in response to internal or external signals, whereby the nucleus becomes one of the targets. The process of nuclear dismantling includes events affecting the nuclear envelope, such as formation of lobes at the nuclear surface, selective proteolysis of nucleoporins, and NPC clustering. In addition, chromatin condensation increases in coordination with DNA fragmentation. However, according to these authors, the process of NPC disassembly undergoing PCD in plants is still poorly understood. So far, our results allow us to describe the ultrastructural characteristics of TCs and SCs undergoing PCD during *A. angustifolia* SE development.

Based on morphological characteristics, our results allow us to propose, for the first time, a fate map of *A. angustifolia* SE development, as shown in Fig. 9. Somatic embryogenesis in *A. angustifolia* consists of a series of steps that include induction and proliferation of embryogenic cultures composed of proembryogenic masses (PEMs) that precede early SE formation. From the induction step, PEMs proliferate through three specific developmental stages, PEM I, II, and III, as represented by changes in the number of embryogenic cells, including ECs and SCs. PEMs characterize the proembryogenic stage which involves all stages before the elongation of the suspensor, similar to that observed in ZE development. This step is promoted in culture medium, either with or without the addition of PGRs (Santos et al. 2002; Silveira et al. 2002; Steiner et al. 2005, 2007). At the proembryogenic stage, the priority seems to be the proliferation of PEMs, while at early stage, the rearrangement of ECs and SCs into two different poles was observed to give rise to an organized structure. The starting point of PEM III-to-early SE transition in *A. angustifolia* occurs at the prematuration step. The trigger of this process is the withdrawal of PGRs of culture medium, followed by FLD preculture with maltose and PEG supplementation of the culture medium (Farias-Soares et al. 2014). Early SEs arise when compact clusters of ECs grow out from PEM III. Based on these observations, two regions were revealed: the dense globular embryonic mass (EM) in the apical part and the SR in the basal part. At this stage, the presence of a cell layer was observed between ECs and SCs composed of TCs. In this sequence, the maturation step is launched whereby early SE progresses to late SE. The formation of late SE is stimulated when the early SE receives chemical signals specific to osmotic and hormonal adjustment during the maturation step (Steiner et al. 2008). The morphology of the late SE stage was not analyzed in the present work; however, previous work carried out by our research group reported that a low number of late SE was obtained (Steiner et al. 2008). According to these authors, this could have resulted from early SE exposure to ABA treatments before reaching the appropriate developmental stage, similar to that described for SEs of *Picea abies* (Filonova et al. 2002; von Arnold et al. 2002). Based on this result, recent works reported the inclusion of the prematuration step in somatic embryogenesis protocols in order to promote the progression from PEM III to early SE (Vieira et al. 2012; Farias-Soares et al. 2014). Based on the knowledge gained from studying the developmental pathway of somatic embryogenesis in this species, a morphogenic model system can be proposed. In this sense, the morphological characterization

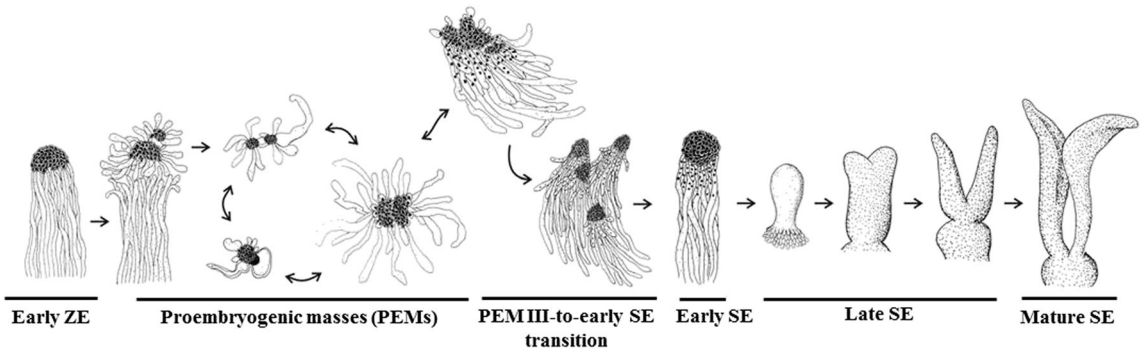

Fig. 9 Schematic representation of the fate map of somatic embryo (SE) development in *Araucaria angustifolia*. In the induction step, embryogenic culture is originated from the apical part of early zygotic embryo (ZE). Embryogenic cultures are represented by proliferation of proembryogenic masses (PEMs) which progresses under specific signals through three characteristic stages distinguished by cellular and morphological organization: PEM I, II, and III. PEMs are composed of a group of embryogenic cells (ECs) connected to a group of suspensor-like-cells (SCs). Before progressing from PEM to SE, changes in morphological organization and polarity establishment of the PEM are required. The PEM III-to-early SE transition is characterized by a compact cluster of ECs growing out of PEM III, albeit still connected to it by SCs, with polarity being observed. After transition, early SEs are characterized by individualized structures composed of dense globular embryonic masses (EM) connected to a suspensor region (SR). Once early somatic embryos are formed, their further development to mature development follows a stereotypical sequence of stages as described for zygotic embryogenesis (Singh 1978). Induction and proliferation are performed in the presence or absence of PGRs (auxins, cytokinins, and polyamines) (Santos et al. 2002; Steiner et al. 2005, 2007). The trigger for the transition of PEMs is the withdrawal of PGRs of culture medium, followed by FLD preculture with maltose and PEG supplementation to the culture medium (Farias-Soares et al. 2014). Finally, late and mature embryos develop in the presence of ABA (Steiner et al. 2008)

and identification of *A. angustifolia* proembryogenic and early SE stages performed in this work can be useful to select cell lines and appropriate culture conditions to improve the somatic embryogenesis protocol. Moreover, this study shows the cell biology of SE development of this particular and primitive gymnosperm, and this could also be useful to evolutionary studies in this area. Finally, we suggest that the improvement of somatic embryogenesis protocol of this species, in association with cryopreservation techniques, becomes a powerful tool to promote the ex situ conservation of this endangered Brazilian native conifer.

Acknowledgments The authors acknowledge the staff of the Central Laboratory of Electron Microscopy (LCME) of the Federal University of Santa Catarina, Florianópolis, Santa Catarina, Brazil. This study was supported by Conselho Nacional de Desenvolvimento Científico e Tecnológico (CNPq, Brazil) and the Fundação de Apoio à Pesquisa Cientifica e Inovação Tecnológica do Estado de Santa Catarina (FAPESC).

Conflict of interest The authors declare that they have no conflict of interest.

References

Abrahamsson M, Valadares S, Larsson E, Clapham D, von Arnold S (2012) Patterning during somatic embryogenesis in Scots pine in relation to polar auxin transport and programmed cell death. Plant Cell Tissue Organ Cult 109:391–400

Astarita LV, Guerra MP (1998) Early somatic embryogenesis in *Araucaria angustifolia* —induction and maintenance of embryonal-suspensor mass cultures. Braz J Plant Physiol 10:113–118

Baker CN, Banerjee SN, Tenover FC (1994) Evaluation of alamar colorimetric MIC method for antimicrobial susceptibility testing of gram-negative bacteria. J Clin Microbiol 32:1261–1267

Balbuena TS, Silveira V, Junqueira M, Dias LLC, Santa-Catarina C, Shevchenko A, Floh EIS (2009) Changes in the 2-DE protein profile during zygotic embryogenesis in Brazilian Pine (*Araucaria angustifolia*). J Proteome 72:337–352

Dodeman VL, Ducreux G, Kreis M (1997) Zygotic embryogenesis versus somatic embryogenesis. J Exp Bot 48:1493–1509

Dogra PD (1978) Morphology, development and nomenclature of conifer embryo. Phytomorphology 28:307–322

Domínguez F, Cejudo FJ (2012) A comparison between nuclear dismantling during plant and animal programmed cell death. Plant Sci 197: 114–121

Durzan DJ (2008) Monozygotic cleavage polyembryogenesis. Cytol Genet 42:159–173

Dutra NT, Silveira V, de Azevedo IG, Gomes-Neto LR, Façanha AR, Steiner N, Guerra MP, Floh EIS, Santa-Catarina C (2013) Polyamines affect the cellular growth and structure of pro- embryogenic masses in *Araucaria angustifolia* embryogenic cultures through the modulation of proton pump activities and endogenous levels of polyamines. Physiol Plant 148:121–132

Elbl PM, Lira BS, Andrade SCS, Jo L, Santos ALW, Coutinho LL, Floh EIS, Rossi MM (2015) Comparative transcriptome analysis of early somatic embryo formation and seed development in Brazilian pine *Araucaria angustifolia* (Bertol.) Kuntze. Plant Cell Tissue Organ Cult 120:903–915

Farias-Soares FL, Burrieza HP, Steiner N, Maldonado S, Guerra MP (2013) Immunoanalysis of dehydrins in *Araucaria angustifolia* embryos. Protoplasma 250:911–918

Farias-Soares FL, Steiner N, Schmidt EC, Pereira MLT, Rogge-Renner GD, Bouzon ZL, Floh EIS, Guerra MP (2014) The transition of proembryogenic masses to somatic embryos in *Araucaria angustifolia* (Bertol.) Kuntze is related to the endogenous contents of IAA, ABA and polyamines. Acta Physiol Plant 36:1853–1865

Filonova LH, Bozhkov PV, von Arnold S (2000a) Developmental pathway of somatic embryogenesis in *Picea abies* as revealed by time-lapse tracking. J Exp Bot 51:249–264

Filonova LH, Bozhkov PV, Brukhin VB, Daniel G, Zhivotovsky B, von Arnold S (2000b) Two waves of programmed cell death occur during formation and development of somatic embryos in the gymnosperm, Norway spruce. J Cell Sci 113:4399–4411

Filonova LH, Von Arnold S, Daniel G, Bozhkov PV (2002) Programmed cell death eliminates all but one embryo in a polyembryonic plant seed. Cell Death Differ 9:1057–1062

Gahan PB (1984) Plant histochemistry and cytochemistry: an introduction. Academic, London

Gärtner PJ, Nagl W (1980) Acid phosphatase activity in plastids (plastolysomes) of senescing embryo-suspensor cells. Planta 149: 341–349

Geburek T, Konrad H (2008) Why the conservation of forest genetic resources has not worked. Conserv Biol 22:267–274

Global Strategy for Plant Conservation. The targets 2011–2020 https://www.cbd.int/gspc/targets.shtml. Accessed 01 Oct 2014

Gordon EM, McCandless EL (1973) Ultrastructure and histochemistry of *Chondrus crispus* Stack. Proc Nova Scotian Inst Sci 27:111–133

Grigová M, Kubeš M, Drážná N, Øezanka T, Lipavská H (2007) Storage lipid dynamics in somatic embryos of Norway spruce (*Picea abies*): histochemical and quantitative analyses. Tree Physiol 27:1533–1540

Guerra MP, Silveira V, Santos ALW, Astarita LV, Nodari RO (2000) Somatic embryogenesis in *Araucaria angustifolia* (Bert) O. Ktze. In: Jain SM, Gupta PK, Newton RJ (eds) Somatic embryogenesis in woody plants. Kluwer Academic Press, Dordrecht, pp 457–478

Guerra MP, Steiner N, Mantovani A, Nodari RO, Reis MS, dos Santos KL (2008) Evolução, ontogênese e diversidade genética em *Araucaria angustifolia*. In: Barbieri RL, Stumpf ERT (eds) Origem e evolução de plantas cultivadas. Embrapa Inf Tecnol, Brasilia, DF, pp 149–184

Gupta PK, Durzan DJ (1987) Somatic embryos from protoplasts of loblolly pine proembryonal cells. Nat Biotechnol 5:710–712

Gupta PK, Pullman GS (1991) Method for reproducing coniferous plants by somatic embryogenesis using abscisic acid and osmotic potential variation. US Patent 5:36–37

Hayat MA (1978) Introduction to biological scanning electron microscopy. University Park Press, Baltimore

Haywood V, Kragler F, Lucas WJ (2002) Plasmodesmata: pathways for protein and ribonucleoprotein signaling. The Plant Cell S303–S325

Helmersson A, von Arnold S (2009) Embryogenic cultures of *Juniperus communis*; easy establishment and embryo maturation, limited germination. Plant Cell Tissue Organ Cult 96:211–217

Helmersson A, von Arnold S, Bozhkov PV (2008) The level of free intracellular zinc mediates programmed cell death/cell survival decisions in plant embryos. Plant Physiol 147:1159–1167

International Union of Conservation of Nature Red List of Threatened Species (2013) http://www.iucnredlist.org/search. Accessed 02 Oct 2013

Jaskowiak MA (2014) Reviews of science for science librarians: the conservation of endangered plants using micropropagation. Sci Technol Libr 33:1

Jo L, Dos Santos ALW, Bueno CA, Barbosa HR, Floh EIS (2013) Proteomic analysis and polyamines, ethylene and reactive oxygen species levels of *Araucaria angustifolia* (Brazilian pine) embryogenic cultures with different embryogenic potential. Tree Physiol 34:94–104

Joy RW, Yeung EC, Kong L, Thorpe TA (1991) Development of white spruce somatic embryos: I. Storage product deposition. In Vitro Cell Dev Biol Plant 27:32–41

Khuri S, Shmoury MR, Baalbaki R, Maunder ME, Talhouk SN (2000) Conservation of the *Cedrus libani* populations in Lebanon: history, current status and experimental application of somatic embryogenesis. Biodivers Conserv 9:1261–1273

Klionsky DJ, Abdalla FC, Abeliovich H et al (2012) Guidelines for the use and interpretation of assays for monitoring autophagy. Autophagy 8(4):1–100

Kurata T, Okada K, Wada T (2005) Intercellular movement of transcription factors. Curr Opin Plant Biol 8:600–605

Larsson E, Sitbon F, Ljung K, von Arnold S (2008a) Inhibited polar auxin transport results in aberrant embryo development in Norway spruce. New Phytol 177:356–366

Larsson E, Sitbon F, von Arnold S (2008b) Polar auxin transport controls suspensor fate. Plant Signal Behav 3:469–470

Ma X, Bucalo K, Determann RO, Cruse-Sanders JM, Pullman GS (2012) Somatic embryogenesis, plant regeneration, and cryopreservation for *Torreya taxifolia*, a highly endangered coniferous species. In Vitro Cell Dev Biol Plant 48:324–334

Maruyama E, Hosoi Y, Ishii K (2007) Somatic embryogenesis and plant regeneration in yakutanegoyou, *Pinus armandii* Franch. var. *amamiana* (koidz) Hatusima, an endemic and endangered species in Japan. In Vitro Cell Dev Biol Plant 43:28–34

Nagl W (1977) 'Plastolysomes'—plastids involved in the autolysis of the embryo-suspensor in *Phaseolus*. Z Pflanzenphysiol 85:45–51

Ouriques LC, Bouzon ZL (2008) Organização estrutural e ultra-estrutural das células vegetativas e da estrutura plurilocular de *Hincksia mitchelliae* (Harvey) P C Silva (Ectocarpales, Phaeophyceae). Rodriguesia 59:435–447

Pullman GS, Bucalo K (2011) Pine somatic embryogenesis using zygotic embryos as explants. Methods Mol Biol 710:267–291

Pullman GS, Johnson S, Peter G, Cairney J, Xu N (2003) Improving loblolly pine somatic embryo maturation: comparison of somatic and zygotic embryo morphology, germination, and gene expression. Plant Cell Rep 21:747–758

Rogge-Renner GD, Steiner N, Schmidt EC, Bouzon ZL, Farias FL, Guerra MP (2013) Structural and component characterization of meristem cells in *Araucaria angustifolia* (Bert.) O. Kuntze zygotic embryo. Protoplasma 250:731–739

Santa-Catarina C, Silveira V, Steiner N, Guerra MP, Floh EIS, dos Santos ALW (2013) The use of somatic embryogenesis for mass clonal propagation and biochemical and physiological studies in woody plants. Curr Top Plant Biol 13:103–119

Santos ALW, Silveira V, Steiner N, Vidor M, Guerra MP (2002) Somatic embryogenesis in Paraná Pine (*Araucaria angustifolia* (Bert.) O. Kuntze). Braz Arch Biol Technol 45:97–106

Schlögl PS, dos Santos ALW, do Nascimento Vieira L, Floh EIS, Guerra MP (2012) Gene expression during early somatic embryogenesis in Brazilian pine (*Araucaria angustifolia* (Bert) O. Ktze). Plant Cell Tissue Organ Cult 108:173–180

Schmidt EC, dos Santos R, Horta PA, Maraschin M, Bouzon ZL (2010) Effects of UVB radiation on the agarophyte *Gracilaria domingensi*s (Rhodophyta, Gracilariales): changes in cell organization, growth and photosynthetic performance. Micron 41:919–930

Schmidt EC, Pereira B, Pontes CLM, Santos R, Scherner F, Horta PA, Paula MR, Latini A, Maraschin M, Bouzon ZL (2012) Alterations in architecture and metabolism induced by ultraviolet radiation-B in the carragenophyte *Chondracanthus teedei* (Rhodophyta, Gigartinales). Protoplasma 249:353–367

Silveira V, Steiner N, Santos ALW, Nodari RO, Guerra MP (2002) Biotechnology tools in *Araucaria angustifolia* conservation and improvement: inductive factors affecting somatic embryogenesis. Crop Breed Appl Biotechnol 2:463–470

Singh H (1978) Embryology of gymnosperms. In: Zimmerman W, Carlquist Z, Ozenda P, Wulff HD (eds) Handbuch der Pflanzen anatomie. Stuttgart, Berlin, pp 187–241

Smertenko AP, Bozhkov PV, Filonova LF, Von Arnold S, Hussey PJ (2003) Re-organization of the cytoeskeleton during developmental programmed cell death in *Picea abies* embryos. Plant J 33:813–824

Souter M, Lindsey K (2000) Polarity and signaling in plant embryogenesis. J Exp Bot 51:971–983

Spurr AR (1969) A low viscosity epoxy resin-embedding medium for electron microscopy. J Ultrastruct Res 26:31–43

Stefenon VM, Steiner N, Guerra MP, Nodari RO (2009) Integrating approaches towards the conservation of forest genetic resources: a case study of *Araucaria angustifolia*. Biodivers Conserv 18:2433–2448

Steiner N, Vieira FN, Maldonado S, Guerra MP (2005) Carbon source affects morphogenesis and histodifferentiation of *A. angustifolia* embryogenic cultures. Braz Arch Biol Technol 48:896–903

Steiner N, Santa-Catarina C, Silveira V, Floh EI, Guerra MP (2007) Polyamine effects on growth and endogenous hormones levels in *Araucaria angustifolia* embryogenic cultures. Plant Cell Tissue Organ Cult 89:55–62

Steiner N, Santa-Catarina C, Andrade JBR, Balbuena TS, Guerra MP, Handro W, Floh EIS, Silveira V (2008) *Araucaria angustifolia* biotechnology. Functional Plant Sci Biotechnol 2:20–28

Steiner N, Santa-Catarina C, Guerra MP, Cutri L, Dornelas MC, Floh EIS (2012) A gymnosperm homolog of SOMATIC EMBRYOGENESIS RECEPTOR-LIKE KINASE-1 (SERK1) is expressed during somatic embryogenesis. Plant Cell Tissue Organ Cult 109:41–50

Tereso S, Zoglauer K, Milhinhos A, Miguel A, Oliveira MM (2007) Zygotic and somatic embryo morphogenesis in *Pinus pinaster*: comparative histological and histochemical study. Tree Physiol 27:661–669

Verdeil JL, Hocher V, Huet C, Grosdemange F, Escoute J, Ferriére N, Nicole M (2001) Ultrastructural changes in coconut calli associated with the acquisition of embryogenic competence. Ann Bot 88:9–18

Verdeil JL, Alemanno L, Niemenak N, Tranbarger TJ (2007) Pluripotent versus totipotent plant stem cells: dependence versus autonomy? Trends Plant Sci 12:245–252

Vieira LN, Santa-Catarina C, Fraga HPF, Santos ALW, Steinmacher DA, Schlogl PS, Silveira V, Steiner N, Floh EIS, Guerra MP (2012) Glutathione improves early somatic embryogenesis in *Araucaria angustifolia* (Bert) O. Kuntze by alteration in nitric oxide emission. Plant Sci 195:80–87

von Arnold S, Clapham D (2008) Spruce embryogenesis. In: Suárez MF, Bozhkov PV (eds). Plant embryogenesis methods in molecular biology. Humana, Totowa, NJ, 427:31–47

von Arnold S, Sabala I, Bozkov P, Dyachok J, Filonova LH (2002) Developmental pathways of somatic embryogenesis. Plant Cell Tissue Organ Cult 69:233–249

von Arnold S, Bozhkov P, Clapham D, Dyachok J, Filonova LH, Hogberg KA, Ingouff M, Wiweger M (2005) Propagation of Norway spruce via somatic embryogenesis. Plant Cell Tissue Organ Cult 1:323–329

Weigel D, Jürgens G (2002) Stem cells that make stems. Nature 415:751–754

Williams CG (2009) Conifer reproductive biology. Springer, New York. doi:10.1007/978-1-4020-9602-0

Winkelmann T (2013) Recent advances in propagation of woody plants. Acta Horticult 990:375–382

Yeung EC (1995) Structural and developmental patterns in somatic embryogenesis. In: Thorpe TA (ed) In vitro embryogenesis in plants. Kluwer, Netherlands, pp 205–247

Yeung EC, Stasolla C, Kong L (1998) Apical meristem formation during zygotic embryo development of white spruce. Can J Bot 76:751–761